

## Supporting Information

### **Boron, Nitrogen and Phosphorous Ternary Doped Graphene Aerogel with Hierarchically Porous Structures as Highly Efficient Electrocatalysts for Oxygen Reduction Reaction**

Hualin Lin,<sup>a,‡</sup> Lei Chu,<sup>a,‡</sup> Xinjing Wang,<sup>a</sup> Zhaoquan Yao,<sup>c</sup> Fan Liu,<sup>a</sup> Yani Ai,<sup>a</sup> Xiaodong Zhuang<sup>\*b</sup> and Sheng Han,<sup>\*a</sup>

*<sup>a</sup>School of Chemical and Environmental Engineering, Shanghai Institute of Technology, Haiquan Road 100, 201418, Shanghai, P. R. China  
Email: hansheng654321@sina.com*

*<sup>b</sup>School of Chemistry and Chemical Engineering, Shanghai Jiao Tong University, Dongchuan Road 800, 200240, Shanghai, P. R. China.  
Email: zhuang@sjtu.edu.cn*

*<sup>c</sup>School of Aeronautics and Astronautics, Shanghai Jiao Tong University, Dongchuan Road 800, 200240, Shanghai, P. R. China.*

*‡*These authors contributed equally to this work.

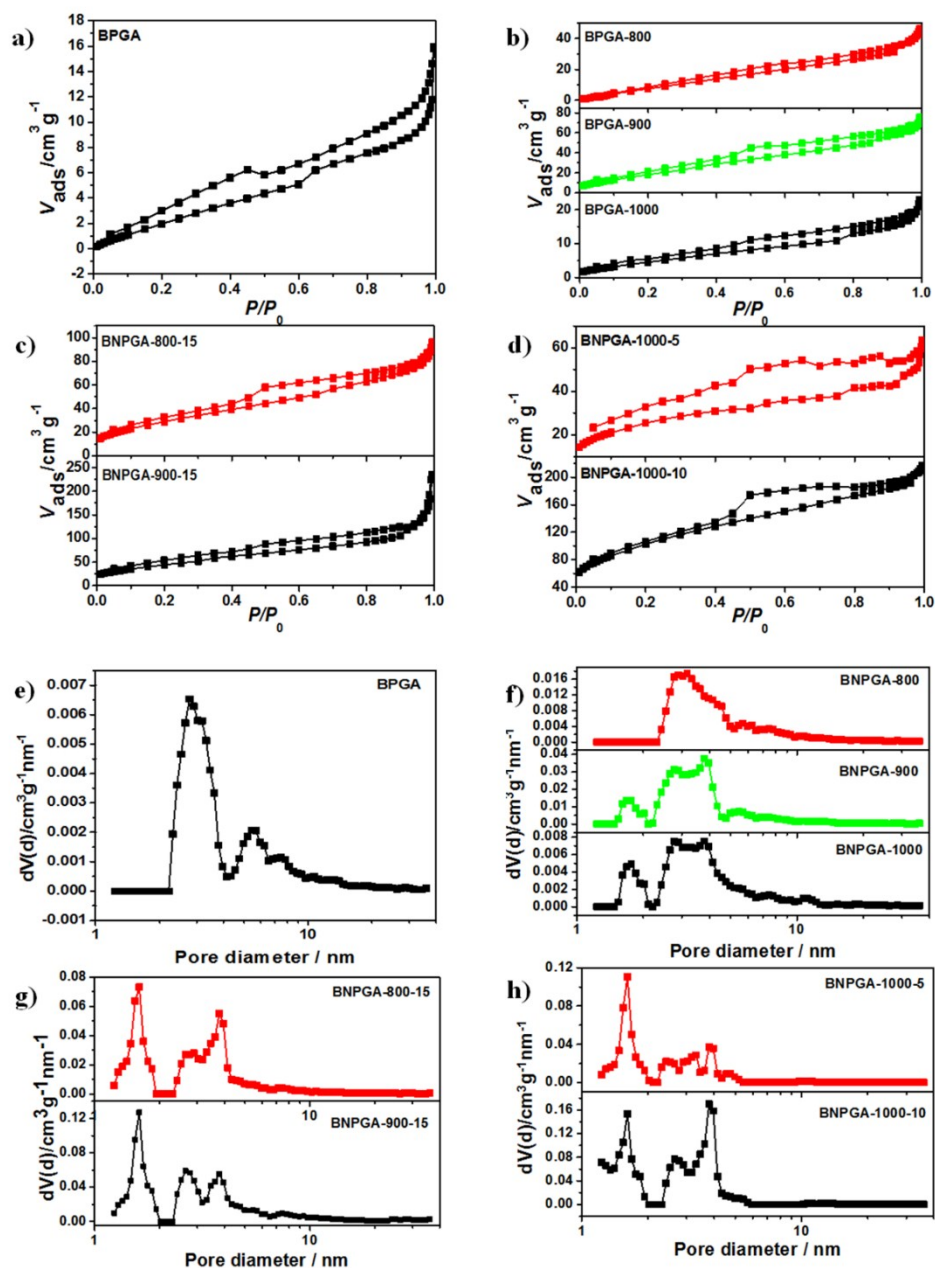


**Fig. S1.** Nitrogen adsorption-desorption isotherms (a), (c), (e), (g) and pore size distributions (b), (d), (f), (h) of BNPGA, BNPGA- $X_1$  ( $X_1=800, 900, 1000$ ), BNPGA-800-15, BNPGA-900-15 and BNPGA-1000-5, BNPGA-1000-10 measured at 77K. Detailed analysis was concluded in **Table 1**.

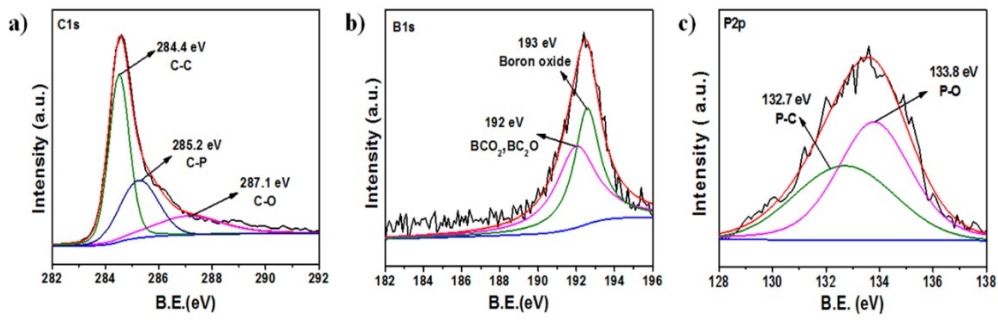


**Fig. S2.** (a) C 1s, (b) B 1s, and (c) P 2p XPS signals for BPGA

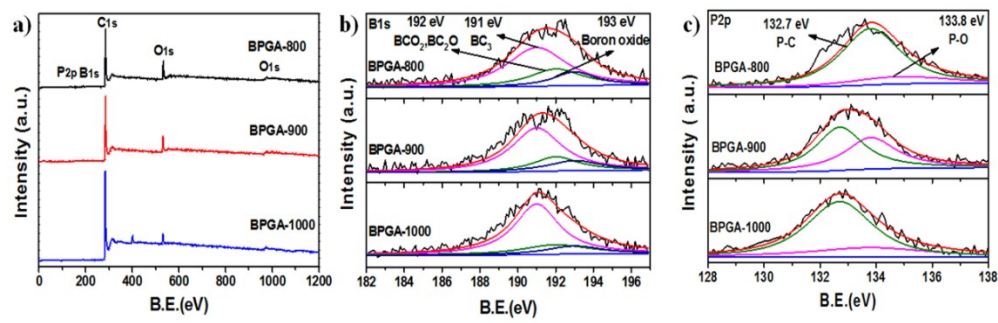


**Fig. S3** (a) XPS survey spectra and (b) B 1s, (c) P 2p XPS signals for BPGA-800, BPGA-900, BPGA-1000.

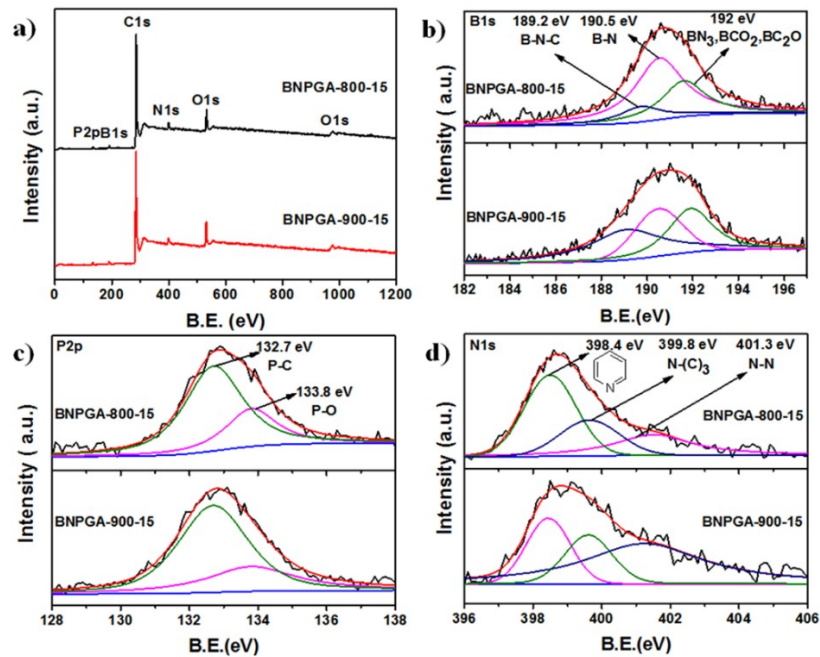


**Fig. S4** (a) XPS survey spectra and (b) B 1s, (c) P 2p, (d) N 1s XPS signals for BNPGA-800-15, BNPGA-900-15.

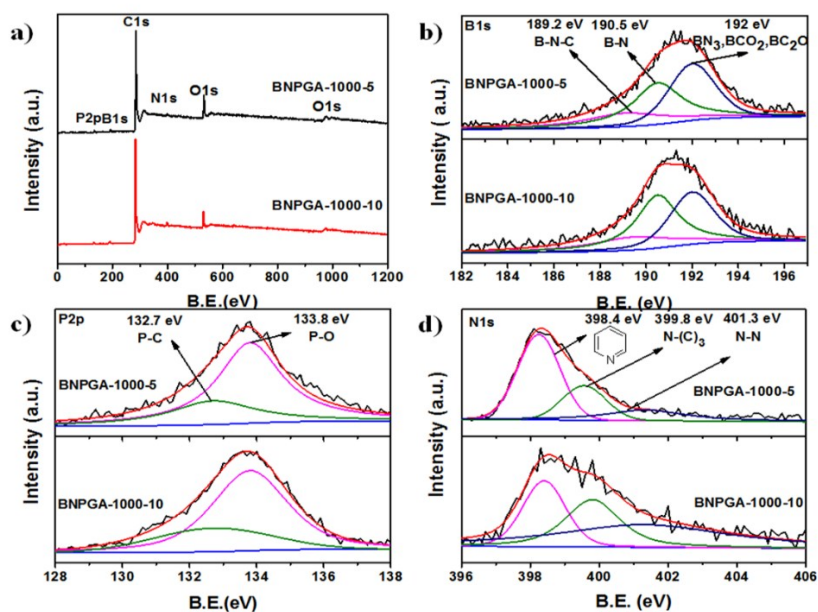


**Fig. S5** (a) XPS survey spectra and (b) B1s, (c) P2p, (d) N1s XPS signals for BNPGA-1000-5, BNPGA-1000-10.

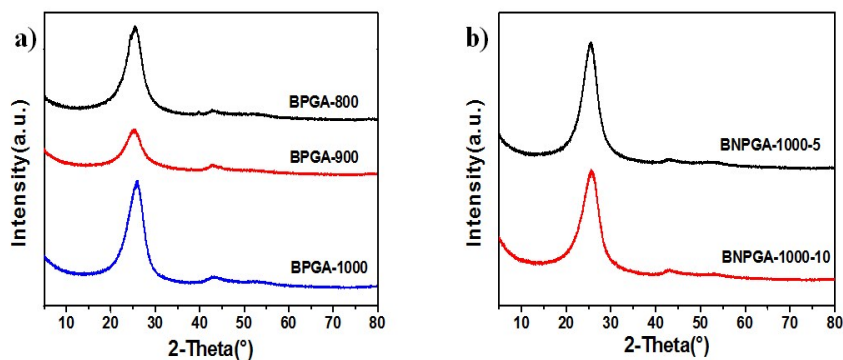


**Fig. S6** XRD patterns of (a) BPGA-800, BPGA-900, BPGA-1000 and (b) BNPGA-1000-5, BNPGA-1000-10.

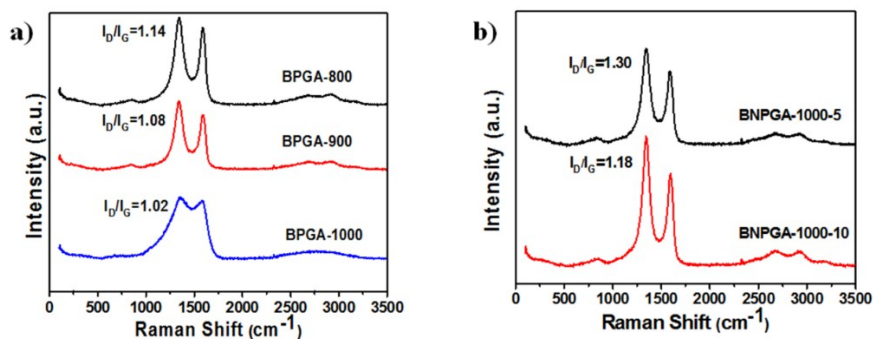


**Fig. S7** Raman spectra of (a) BPGA-800, BPGA-900, BPGA-1000 and (b) BNPGA-1000-5, BNPGA-1000-10.

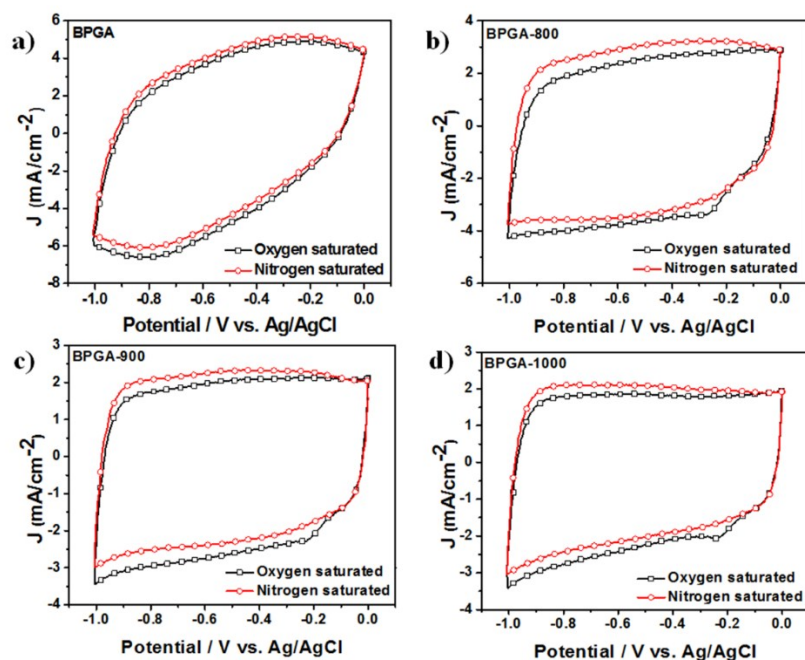


**Fig. S8** Cyclic voltammograms of **(a)** BPGA, **(b)** BPGA-800, **(c)** BPGA-900 and **(d)** BPGA-1000 at a scan rate of  $100 \text{ mV s}^{-1}$  in  $\text{O}_2$  and  $\text{N}_2$ -saturated  $0.1\text{M}$  KOH solution.

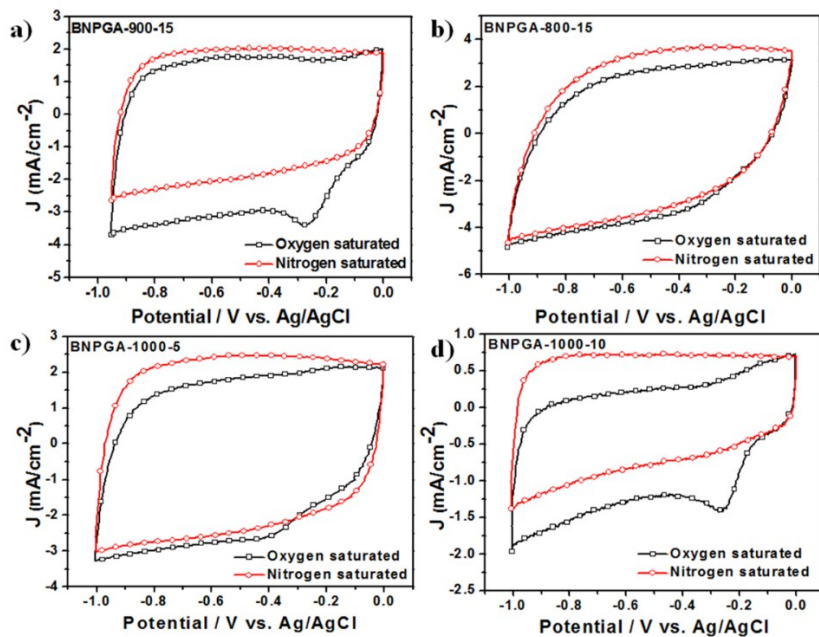


**Fig. S9** Cyclic voltammograms of **(a)** BNPGA-800-15, **(b)** BNPGA-900-15, **(c)** BNPGA-1000-5 and **(d)** BNPGA-1000-10 at a scan rate of  $100 \text{ mV s}^{-1}$  in  $\text{O}_2$  and  $\text{N}_2$ -saturated  $0.1 \text{ M}$  KOH solution.

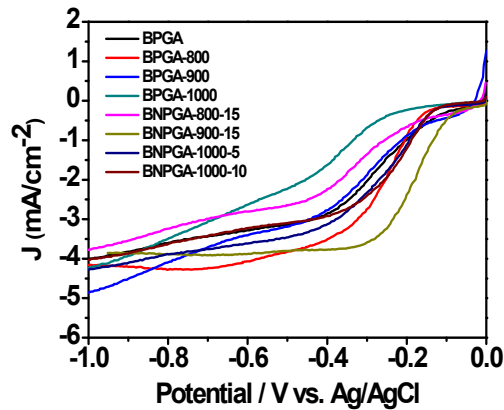


**Fig. S10** LSVs of BPGA, BPGA-X, BNPGA-X-Y and commercial Pt/C at a rotation rate of 1600 rpm with a scan rate of  $10 \text{ mV s}^{-1}$  in  $\text{O}_2$ -saturated 0.1 M KOH solution

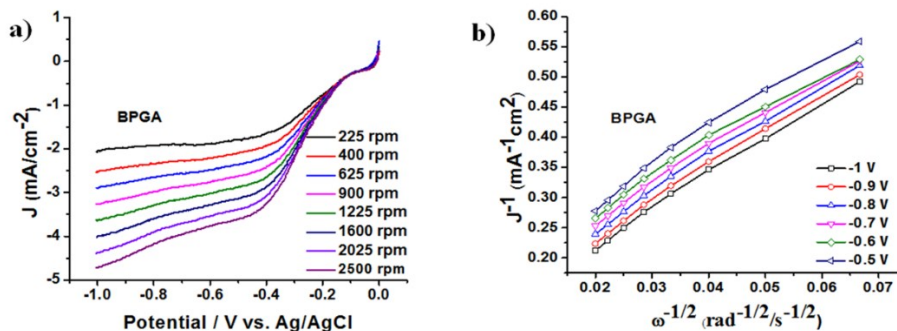


**Fig. S11 (a)** RDE voltammograms of BNPGA at different rotating speeds with a scan rate of  $10 \text{ mV s}^{-1}$  in  $\text{O}_2$ -saturated 0.1 M KOH solution. **(b)** Koutecky–Levich plots of  $j^{-1}$  versus  $\omega^{-1/2}$  of the BNPGA at potentials of -0.5, -0.6, -0.7, -0.8, -0.9 and -1.0 V.

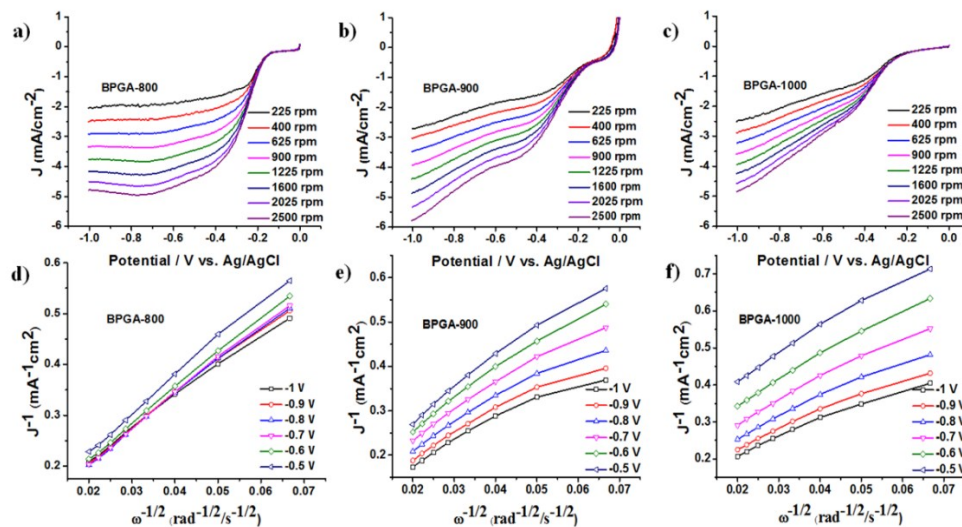


**Fig. S12 (a), (b), (c)** RDE voltammograms of BPGA-800, BPGA-900 and BPGA-1000 at different rotating speeds with a scan rate of  $10 \text{ mV s}^{-1}$  in  $\text{O}_2$ -saturated 0.1 M KOH solution. **(d), (e), (f)** Koutecky–Levich plots of  $j^{-1}$  versus  $\omega^{-1/2}$  of the BPGA-800, BPGA-900 and BPGA-1000 at potentials of -0.5, -0.6, -0.7, -0.8, -0.9 and -1.0 V.

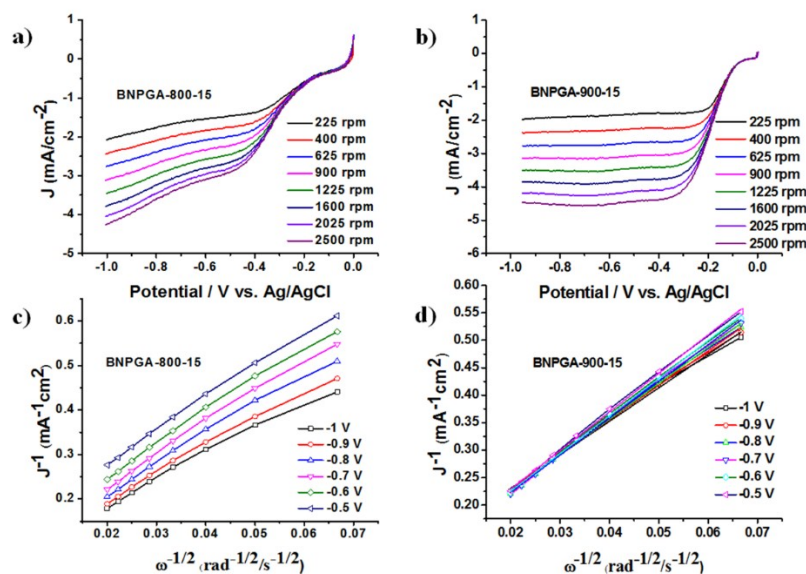


**Fig. S13** (a), (b) RDE voltammograms of BNPGA-800-15 and BNPGA-900-15 at different rotating speeds with a scan rate of  $10 \text{ mV s}^{-1}$  in  $\text{O}_2$ -saturated  $0.1 \text{ M KOH}$  solution. (c), (d) Koutecky–Levich plots of  $j^{-1}$  versus  $\omega^{-1/2}$  of the BNPGA-800-15 and BNPGA-900-15 at potentials of  $-0.5$ ,  $-0.6$ ,  $-0.7$ ,  $-0.8$ ,  $-0.9$  and  $-1.0 \text{ V}$ .

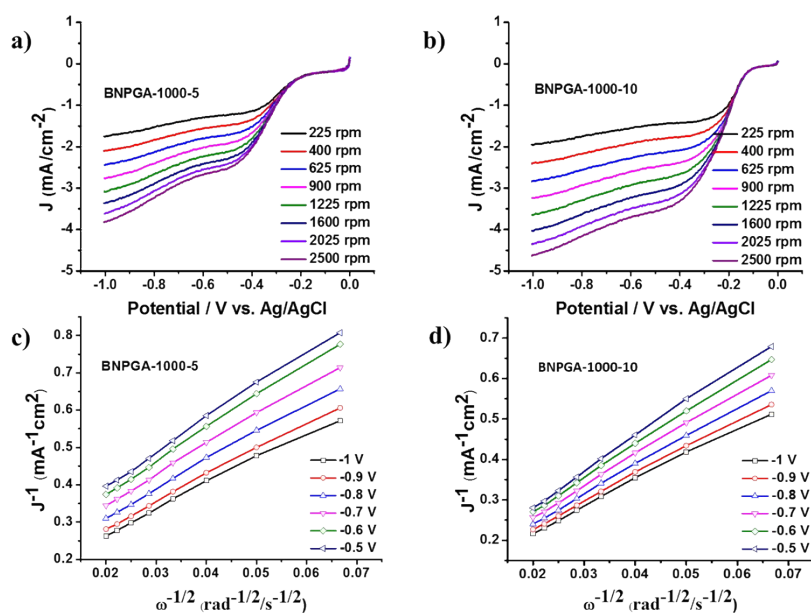


**Fig. S14** (a), (b) RDE voltammograms of BNPGA-1000-5 and BNPGA-1000-10 at different rotating speeds with a scan rate of  $10 \text{ mV s}^{-1}$  in  $\text{O}_2$ -saturated  $0.1 \text{ M KOH}$  solution. (c), (d) Koutecky–Levich plots of  $j^{-1}$  versus  $\omega^{-1/2}$  of the BNPGA-1000-5 and BNPGA-1000-10 at potentials of  $-0.5$ ,  $-0.6$ ,  $-0.7$ ,  $-0.8$ ,  $-0.9$  and  $-1.0 \text{ V}$ .

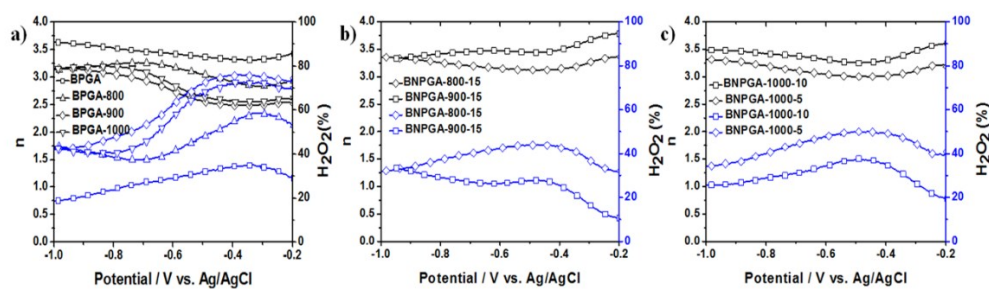


**Fig. S15** The calculated electron transfer numbers ( $n$ ) and percentage of  $H_2O_2$  of **(a)** BPGA, BPGA-800, BPGA-900, BPGA-1000, **(b)** BNPGA-800-15, BNPGA-900-15 and **(c)** BNPGA-1000-5, BNPGA-1000-10.

**Table S1.** Elemental analysis based on XPS analysis.

Samples	C	O	B	N	P	B/C	N/C	P/C
	Weight content (%)							
BPGA	70.99	20.73	4.90	-	3.38	0.07	-	0.05
BPGA-800	77.42	12.10	5.39	-	5.09	0.07	-	0.07
BPGA-900	82.01	10.29	4.02	-	3.68	0.05	-	0.04
BPGA-1000	91.05	4.87	2.12	-	1.97	0.02	-	0.02
BNPGA-800-15	82.26	8.03	3.81	2.83	3.07	0.05	0.03	0.04
BNPGA-900-15	81.97	8.15	4.05	2.17	3.66	0.05	0.03	0.04
BNPGA-1000-15	77.70	8.10	6.53	4.50	3.17	0.08	0.06	0.04
BNPGA-1000-10	82.70	7.59	3.73	2.18	3.80	0.05	0.03	0.04
BNPGA-1000-5	79.14	10.43	5.02	1.98	3.43	0.06	0.03	0.04